Electron transfer and H_2 evolution in hybrid systems based on [FeFe]-hydrogenase anchored on modified TiO_2.

Valeria Polliotto,[a] Simone Morra,[b] Stefano Livraghi,[a] Francesca Valetti,[b] Gianfranco Gilardi,[b] Elio Giamello*[a]

a) *Department of Chemistry and NIS, University of Torino, 10125, Torino, Italy*

b) *Department of Life Sciences and Systems Biology, University of Torino, 10123, Torino, Italy*

* elio.giamello@unito.it

Keywords: EPR, [FeFe]-hydrogenase, doped-TiO_2, H_2 evolution, electron transfer

Abbreviations: EPR, electron paramagnetic resonance; TEOA, triethanolamine; N-TiO_2, N-doped TiO_2; rd- TiO_2, reduced TiO_2; XRD, X-ray diffraction; H_{ox}, H_{ox}-CO EPR detectable species of H-cluster of the protein.

Abstract

An efficient conversion of solar energy into renewable fuels is one of the most important targets in the last decades. The hybrid system composed by [FeFe]-hydrogenase anchored to the surface of TiO_2 could be a valid alternative to typical noble metal co-catalyst in the H_2 production from solar light. In this paper we investigate by Electron Paramagnetic Resonance the interaction of hydrogenase with the surface of three distinct types of TiO_2 anatase, namely the bare oxide, the N-doped one and a substoichiometric blue material (TiO_2-x). Experiments in dark and under irradiation show that the anchored enzyme is in electronic contact with the solid. The catalytic activity under solar light of the three hybrid systems has been preliminary evaluated. The production of H_2 is higher for the system containing N-TiO_2 with respect to that based on the bare oxide indicating a role of the N intra band gap states in harvesting the visible components of sunlight. The system containing reduced TiO_2, in spite of its strong absorption in the visible, is less active suggesting that specific centers for visible light absorption are needed to obtain an efficient photoexitation process.

1. Introduction

Since the discovery, in 1972, of the photosplitting of water in hydrogen and oxygen [1] based on a photo-electrochemical cell with an anode made of titanium dioxide, this compound became a system of reference in the area of photochemical and photo-electrochemical applications. Titanium dioxide,

or titania, is nowadays the most important photocatalyst employed in processes for pollutants abatement,[2] as biocide,[3, 4] in odour control [5] and in self-cleaning of glasses or of external surfaces.[6] As to the mentioned applications for hydrogen production from water, the advent of more efficient (but often much more expansive) materials and of complex approaches both for the preparation of photoelectrodes and for the direct photocatalytic water splitting,[7, 8] eclipsed for quite a long time the role initially played by titania. This material, which has the great advantage to be cheap, abundant and non toxic, actually shows some serious drawbacks hampering its direct use in the process of water photosplitting. The first one is the large value of the TiO_2 band gap (around 3.2 eV for the anatase polymorph) that implicates the use of UV photons to perform the excitation of electrons from the valence band to the conduction band limiting therefore the use of sun light (poor of UV components at the earth surface) in photochemical applications of this material. The second drawback is the electrochemical potential of the conduction band electrons which is only slightly more negative than the H^+/H_2 potential thus limiting the reductive capability of photoexcited electrons. For this reason the most successful photocatalytic applications of titania are in the field of oxidation (e.g. pollutants remediation) so exploiting the excellent oxidative potential of the valence band holes.[9]

The need of overcoming these two serious constraints is at the origin of a long activity aiming to modify the solid in order to improve its performances. Among the methods to adjust the photochemical properties of titania extending to the visible range its optical absorption, it is worth mentioning: i) the grafting of sensitizers at the surface of the solid [10] analogous to what done for Dye Sensitized Solar Cells (DSSC, photovoltaic applications); ii) the use of supported metal nanoparticles (mainly Au) to exploit light absorption due to plasmonic effect;[11, 12] iii) the doping of the solid with various dopants. In the latter case the most intriguing case is that of doping with non-metals. In particular doping with nitrogen [13-16] or with combination of elements including nitrogen [17, 18] has been the object of intense research activity and of warmly debated results. As a matter of fact, nitrogen doped titania is now currently used in photocatalytic applications employing visible light.[19-21]

On the other hand, as far as the production of hydrogen by reduction is concerned, the use of co-catalysts is necessary to overcome the described potential limitation. In this case, beside the use of typical noble metal hydrogenation catalyst like Pt nanoparticles, a particularly interesting approach is the use of a biocatalyst such as hydrogenase. In particoular, the [FeFe]-hydrogenase enzyme is known to catalyse the reversible reduction of H^+ ions to H_2 and its action is due to an iron based catalytic center called H-cluster which is composed by two subclusters, an iron sulphur cubane [4Fe-4S] and a [2Fe] subcluster. The latter is based on an iron pair coordinated by two bridging sulphur

atoms belonging to an organic ligand and by various non-protein ligands, namely three CO and two CN- groups (Figure 1). Furthermore, this protein contains several [FeS] clusters, with suitable redox potentials allowing the electron transfer from an external electron donor to the H-cluster, where the electrons combine with protons to form di-hydrogen molecules.[22-25]

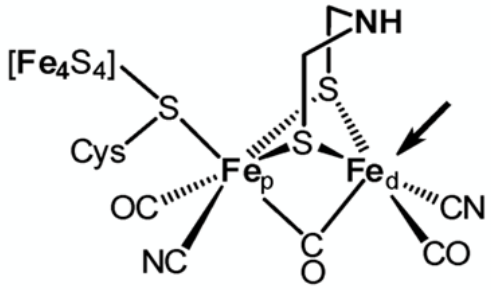

Figure 1. Structure of the H-cluster active site of [FeFe]-hydrogenase; the arrow indicates the open metal coordination site. **(single column fitting image)**

Quite recently hydrogenase-TiO_2 nanohybryds have been prepared and tested in photocatalytic process for hydrogen production based on solar light conversion.[26-32]

The purpose of the present work is to investigate the hybrids prepared coupling hydrogenase with modified titanias. The latter are materials based on the anatase polymorph modified in order to make them capable of absorbing visible light. In particular we employed, comparing the results with those of a sample of bare anatase, two kind of materials: i) N-doped anatase, a yellow material, and ii) a substoichiometric reduced anatase which shows a deep blue colour. In N-doped TiO_2 the presence of nitrogen defects in the lattice of the oxide generates intra band gap energetic levels available to excite the electrons of the valence band to the conduction band under visible light. These states cause the yellow colour of the powder.[13-15, 33]

The substoichiometric TiO_2 is prepared via a particular synthetic route that lead to a partially reduced, blue-colored oxide (TiO_{2-x}) which is stable in air and shows the presence of stable Ti^{3+} ions. The color in this case is due to the tail of a broad absorption centered in the infrared region and typical of reduced titanias.[34-40]

Our aim is therefore to overcome the two limitations of titania described before, using doped solids, capable of harvesting some visible components of the solar spectrum and coupling them to an efficient enzyme for hydrogen reduction. Our attention is paid not only to the efficiency of the hydrogenase-TiO_2 materials in hydrogen production but also to the mechanism of interaction of the protein with the solid and to the effect of irradiation on the hybrid materials. All this has been monitored by Electron Paramagnetic Resonance (EPR). This technique has been widely used in recent years to investigate the active sites of hydrogenase which are, in particular redox states, paramagnetic.[41-45]

EPR, however, has also been used to characterise the paramagnetic centers present in titanium dioxide. In particular the process of photo-induced charge separation creates an electron and a hole which can be stabilized by the solid or transferred from its surface to an adsorbed molecule always producing paramagnetic states.[46-48] The EPR technique is therefore much suited to follow the process occurring in the hydrogenase-TiO_2 system both in dark and under irradiation.

The EPR experiments of the present work have been performed in aqueous solutions containing thionine and triethanolamine (TEOA). TEOA molecule acts as a buffer and as sacrificial electron donor (or scavenger of the photogenerated holes) for TiO_2.[28] Thionine plays the role of stabilizing agent for the oxidized form of the H-cluster (named H_{ox} state) characterized by a diamagnetic $[4Fe4S]^{2+}$ sub-cluster and a paramagnetic [Fe(I)-Fe(II)] sub-cluster.[43]

In the present paper the results will be organized as follows: firstly the effect of the irradiation on the thionine-TEOA aqueous solution and on the suspension of the various bare supports in the same solution will be monitored by EPR in order to investigate the photoinduced processes in the absence of the enzyme. Then the same approach will be followed for the suspension containing the hydrogenase/oxide nanohybrid. Finally, the hydrogen production ability under solar irradiation of the three hybrid systems in TEOA solution will be compared.

2. Materials and Methods

Hydrogenase preparation: CpHydA [FeFe]-hydrogenase was cloned from *Clostridium perfringens* SM09, recombinantly expressed and purified under strict anaerobic conditions as previously described.[49, 50]

TiO_2 synthesis: The bare TiO_2 anatase (hereafter TiO_2) powder was prepared via sol-gel technique, mixing a solution of 15 mL of titanium(IV) isopropoxide in 15 mL of 2-propanol alcohol to which 16 mL of water were added. The gel was left to age for 15 hours at 290 K and subsequently dried at 343 K. The dried material was calcined in air at 773 K for 1 hour.

The N-doped TiO_2 anatase (hereafter N-TiO_2) powder system was prepared with sol-gel technique mixing a solution of 15 mL of titanium(IV) isopropoxide in 14 mL 2-propanol alcohol with a solution of 0.54 g of NH_4Cl in 8 mL of water. The gel was kept for 15 hours at 290 K and subsequently dried at 343 K. The dried material (slightly yellow) was finally calcined in air at 773 K for 1 hours.

The reduced TiO_2 anatase (hereafter rd-TiO_2) powder was prepared via hydrothermal synthesis: 0.5 g of TiB_2 powder precursor was suspended into 20 mL of aqueous solution of HF (1 M), followed by hydrothermal treatment in a teflon autoclave at 453 K overnight. After the reaction, the product was filtred and washed with deionized water three times to remove dissoluble ionic impurities. Then the sample with a dark blue color was dried at 373 K for 1 h.

Suspensions of TiO_2 powders in TEOA (triethanolamine) 25 mM and thionine 1.39 mM aqueous solution were prepared mixing 4 mg of powder in 1 mL of solution. Each suspension was stirred and 70 μL of suspension were transfered in a EPR tube and gradually frozen at 77 K for EPR measurements.

Hybrid materials preparation: The preparation was carried out under an anoxic nitrogen atmosphere in a glove box (Belle Technology). The enzyme was anaerobically concentrated to 0.36 mM using Amicon Ultra 0.5 mL 30K MWCO (Millipore). 8 mg of the TiO_2 powder were suspended and sonicated in 1 mL of the anaerobic buffer 25 mM TEOA pH 7. Subsequently, the enzyme and the TiO_2 suspension were mixed in a 1:1 volume ratio, resulting in final concentrations of 0.18 mM CpHydA and 4 mg/mL TiO_2. Thionine was added to a final concentration of 1.39 mM. 70 μL of this suspension were transferred in a EPR tube, sealed and gradually frozen at 77 K for EPR measurements.

X-Ray Diffraction: Powder X-ray diffraction (XRD) patterns were recorded with a PANalytical PW3040/60 X'Pert PRO MPD diffractometer using a copper Ka radiation source (0.154056 nm). The intensities were obtained in the 2θ range between 20° and 80°. X'Pert High-Score software was used for data handling.

UV-Visible absorbance: The UV-Visible absorption spectra were recorded using a Varian Cary 5 spectrometer, coupled with an integration sphere for diffuse reflectance studies, using a Carywin-UV/scan software. A sample of PTFE with 100% reflectance was used as the reference. Due to the high absorbance of the rd-TiO_2 material, this latter was mixed with a portion of white MgO.

Surface area measurements: The surface area measurements were carried out on a Micromeritics ASAP 2020/2010 apparatus using the Brunauer–Emmett–Teller (BET) model for N_2 adsorption measurements. Prior to the adsorption run, all of the samples were outgassed at 573 K for 3 h.

UV-visible irradiation: All the samples were irradiated with UV-visible light using a 1600 W xenon lamp (Oriel instruments) equipped with a IR water filter. The effect of irradiation on EPR spectra was investigated irradiating the sample in the EPR cavity at 77 K for 15 minutes.

EPR characterization: Continuous Wave Electron paramagnetic resonance (CW-EPR) experiments were performed with a Bruker EMX spectrometer operating at X-band (9.5 GHz), equipped with a cylindrical cavity operating at 100 kHz field modulation. All the spectra were recorded with the following experimental parameters: microwave power 10 mW, Modulation Amplitude 0.2 mT and temperature 77 K.

H_2 photoevolution test: The test was performed in a 7 mL glass vial filled with 1 mL of O_2-free sample solution containing 25 mM TEOA pH 7, 1 mg/mL TiO_2 and 50 nM CpHydA.

They were irradiated for 60 minutes under natural sunlight at a flux of approximately 650 W/m^2. During irradiation the samples were kept on ice. Control experiments in the absence of TiO_2, or the enzyme or in the dark were also performed. All the samples were tested at the same time, under the same experimental conditions.

Hydrogen evolution has been measured via gas chromatography. The gaschromatographer (Agilent Technologies 7890A) was equippedwith purged packed inlet, Molesieve 5A column (30 m, ID 0.53 mm, film 25 μm) and thermal conductivity detector; argon was used as carrier gas. Quantitative separation was achieved in less than 3 min at 60°C.

3. Results and discussion

3.1. Oxide characterization.

XRD analysis were performed on the three distinct polycrystalline systems namely: bare TiO_2, N-TiO_2 and rd- TiO_2. The corresponding XRD patterns are reported in Figure 2a), b) and c) respectively. All the diffraction pattern are characterized by peaks at the same position that correspond to those of the anatase polymorph however, while both TiO_2 and N-TiO_2 exhibit the same linewidth, the pattern of rd- TiO_2 shows much narrower peaks since this oxide possesses significantly larger crystallites. This result is also confirmed by the surface area measurements (BET method), indicating about 80 m^2/g for TiO_2 and N-TiO_2 and about 10 m^2/g for rd-TiO_2.

Figure 3 compares the diffuse reflectance UV-Visible spectra of TiO_2 (black line), N-TiO_2 (red line) and rd-TiO_2 (blue line) powders. The spectra of TiO_2 and N-TiO_2 differ for a slight difference in the band-gap transition and for an absorption shoulder in the visible region centered at about 450 nm and due to intra band gap energy states which is present in the case of N-TiO_2 only (magnification in the inset of Figure 3).[13, 15] At variance, the rd-TiO_2 present a strong continuous absorption in all visible region that is extended also in the NIR and which is typical of substoichiometric materials containing excess electrons either localized on Ti^{3+} centers or delocalized in the conduction band.[34] The band gap values, calculated with the Tauc method, are 3.23 eV and 3.20 eV for TiO_2 and N-TiO_2 respectively and 2.88 eV for rd-TiO_2. These values indicate that the visible absorption and the consequent yellow color of N-TiO_2 sample are due to the absorption shoulder centered at 450nm and not to the band gap transitions which correspond to UV wavelengths. As opposite the band gap transition of rd-TiO_2 oxide occurs in the visible region.

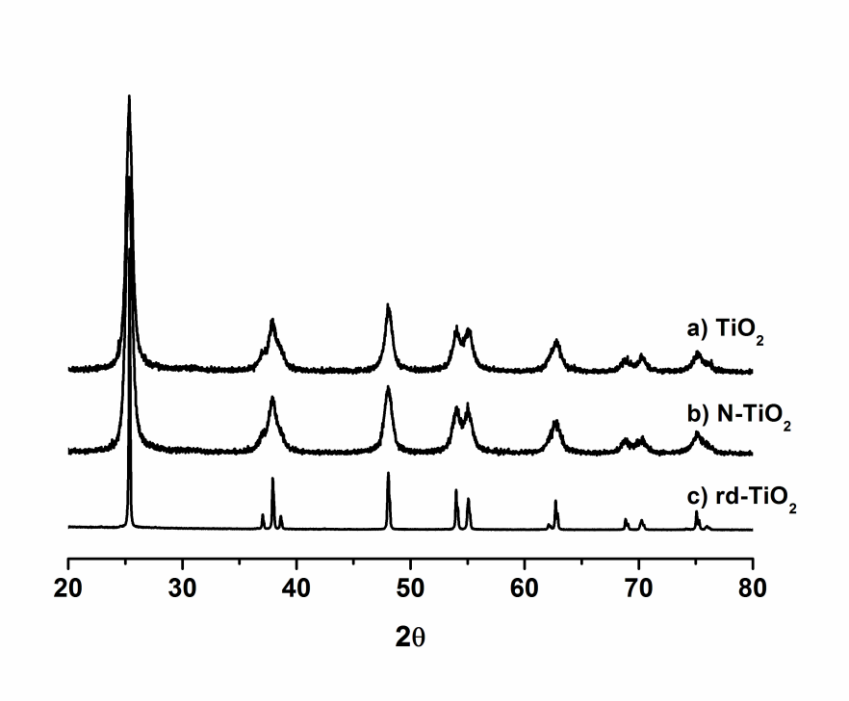

Figure 2. X-ray diffraction patterns of a) TiO_2, b) N-TiO_2 and c) rd-TiO_2 powders. **(single column fitting image)**

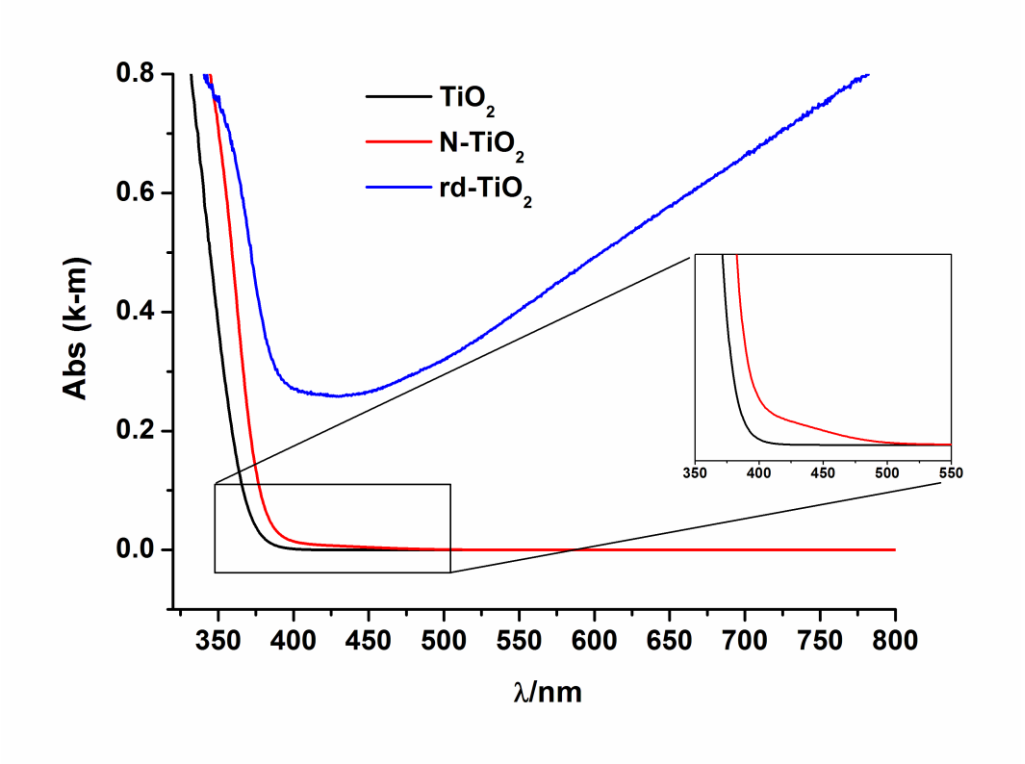

Figure 3. UV-Vis diffuse absorbance spectra of TiO_2 (black line), N-TiO_2 (red line) and rd-TiO_2 (blue line) powders. In the inset a magnification of the visible absorption of N-TiO_2 and TiO_2 is reported. **(single column fitting image)**

3.2. Effect of irradiation on the thionine-TEOA solution.

H_2 production upon irradiation of the various hydrogenase-TiO_2 hybrid systems is based on the light-induced charge separation producing electrons and holes. While the holes are quenched by a suitable scavenger (TEOA in the present case), the electrons are transferred, via the series of Fe-S-clusters,[23, 24] to the active site of the enzyme where the reduction of water protons into molecular hydrogen occurs. The presence of thionine is needed to stabilize the H_{ox} state of protein H-cluster.

A preliminary experiment has been performed to observe, by EPR, the effects of irradiation on the thionine-TEOA solution, in order to understand the possible interference of these molecules with the results of the successive experiments involving irradiation of the hybrid systems. For this experiment a water solution of TEOA (25 mM) and thionine (1.39 mM) was prepared, and gradually frozen at 77K for EPR measurements. Figure 4 shows the effect of the UV-visible irradiation of this thionine solution.

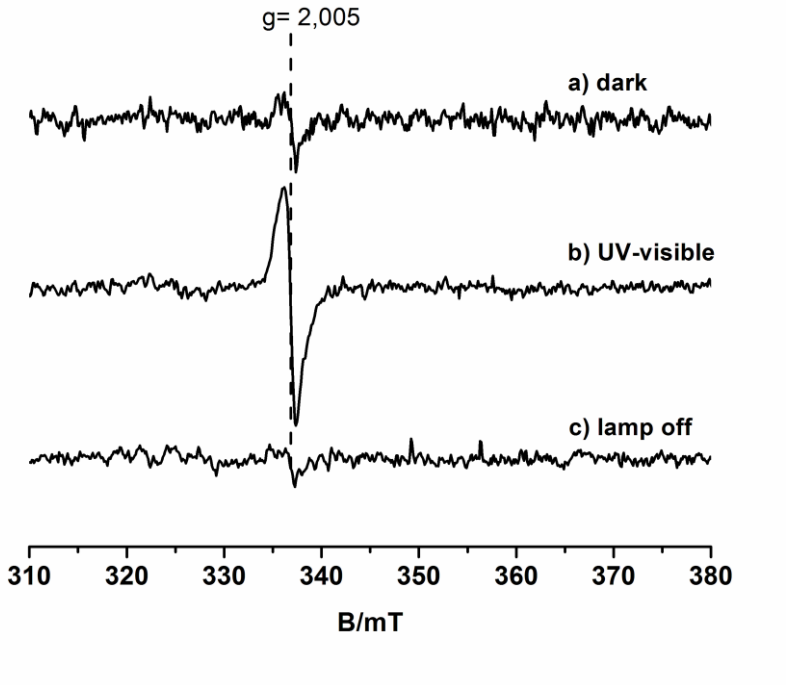

Figure 4. CW-EPR spectra recorded at 77K of the frozen solution containing thionine and TEOA): (a) as prepared solution in dark, (b) sample in (a) under UV-visible irradiation at 77K, (c) the same sample after thaw-freeze treatment (lamp off, heating at RT and cooling again at 77K). **(single column fitting image)**

The spectrum of the as prepared thionine in TEOA solution in dark (Figure 4(a)) shows a very weak, negligible signal centered at g=2.005. This signal however increases upon irradiation (Figure 4(b)) and disappears by heating the sample at room temperature in dark (Figure 4(c)). The isotropic signal

at g=2.005 is due to the formation of small amounts of the thionine radical cation,[51, 52] and is not observed irradiating a solution containing TEOA only. The radical species is stable in the frozen solution only (77K) and is destroyed raising the temperature.

3.3. Irradiation of TiO_2 materials in TEOA-thionine aqueous solution.

Suspensions of the three solid supports (TiO_2, N-TiO_2, rd-TiO_2) employed in this study have been studied by EPR under irradiation in the absence of the surface anchored protein. This preliminary investigation is essential for a comparison with the results of irradiation of the hybrid systems in the same conditions.

The samples have been irradiated under UV-visible light at 77K and the corresponding EPR spectra were recorded at the same temperature. The results are reported in Figure 5 which also reports (spectrum a, for each material) the spectrum of the dry powder prior formation of the suspension.

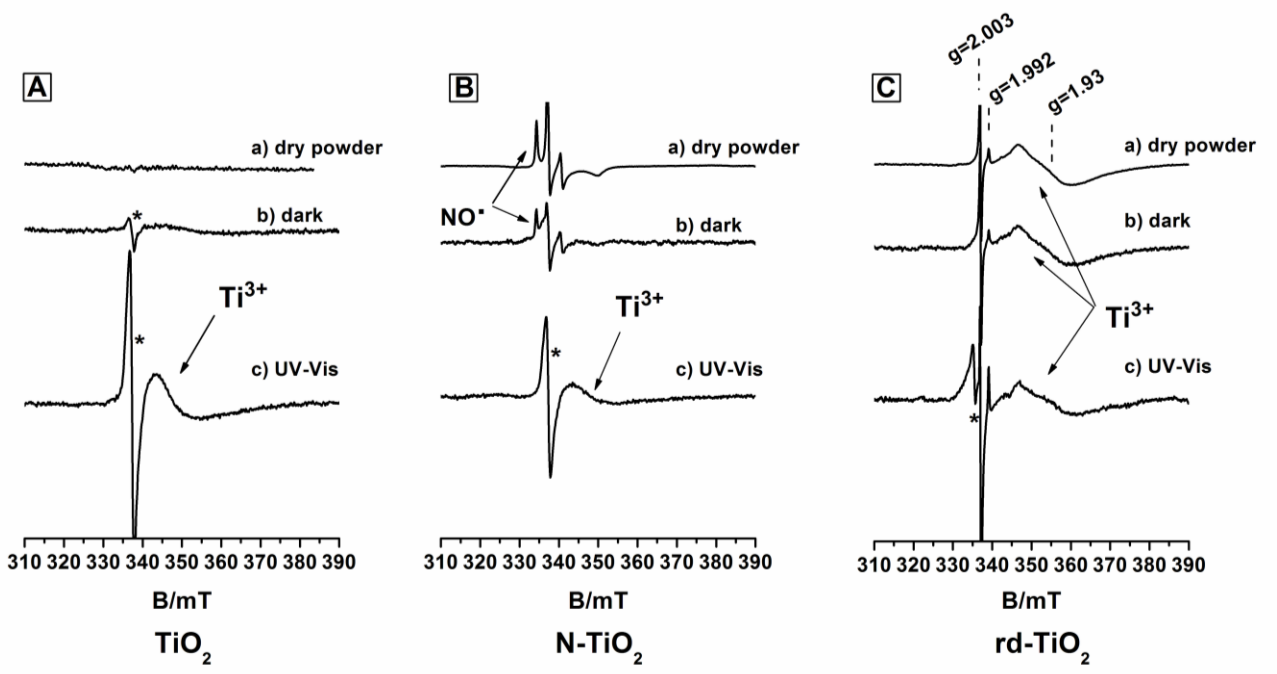

Figure 5. Experimental CW-EPR spectra recorded at 77K of TiO_2 (A), N-TiO_2 (B) and rd-TiO_2 (C) systems recorded under different conditions. (a) powder material in air, (b) frozen suspension of the powder in TEOA-thionine solution; (c) effect of UV-Vis irradiation of the suspension. The asterisk indicates the signal of the thionine radical cation. **(2 columns fitting image)**

The TiO_2 powder in air (Figure 5A(a)) is EPR silent, and also the spectrum of the as prepared TiO_2 suspension in dark (Figure 5A(b)) shows very weak signals including that at g= 2.005, due to the presence of thionine. The irradiation with UV-visible light of the suspension causes a change in the EPR spectrum (Figure 5A(c)) which becomes dominated by the narrow isotropic signal of the irradiated thionine (marked by an asterisk). Beside this signal a broader one, centered at g= 1.93 and

unambiguously due to Ti^{3+} ions in anatase [46] is present. The features of this spectrum are stable after irradiation (lamp off) maintaining the sample at 77K while, after thaw-freeze (RT-77K) (data not shown for sake of brevity), they disappear and the EPR spectrum becomes the same observed (Figure 5A(b)) before irradiation. The effect of the irradiation is therefore clear. Apart for the formation of the thionine radical ion (which is a sort of side-effect of the process and which will be no longer discussed in the following) the experiment indicates that the electrons formed upon irradiation (or, at least, a fraction of them) remain in the solid where they are trapped by Ti^{4+} ions which reduce to Ti^{3+}.[47, 48] The holes photogenareted in parallel are consumed by the electron donor (TEOA) in the system and the classic electron-hole recombination, which would occur increasing the temperature, becomes of course impossible. This is the reason of the formation of the broad signal due to reduced trivalent titanium centers in TiO_2.

The same experiment was performed also for the N-doped and the reduced TiO_2 materials.

In the former case the final result is the same observed for bare TiO_2 as Ti^{3+} centers are observed upon irradiation of the frozen suspension (Figure 5B(c)). The spectra before irradiation are affected by the presence of nitric oxide (NO) which is a by-product of the N-TiO_2 synthesis and which does not interfere with the photochemistry of the material.[15] The typical EPR signal of NO (whose amount is not constant in different samples depending on details of the preparation) is highlighted in Figure 5B(a) and Figure 5B(b) and it is no more visible after irradiation probably because the NO molecule reacts with the photoformed charge carriers.

In the case of the substoichiometric TiO_2 (rd-TiO_2) the spectrum of the powder (Figure 5C(a)) reveals, beside of an isotropic signal at g= 2.003, possibly connected with electron trapped at lattice defects, signals with g values between 1.99-1.88 typical of Ti^{3+} ions in anatase.[46, 47] In particular a narrow signal centered at g=1.992 and a broader one at g=1.93 are visible, respectively due to isolated Ti^{3+} in regular position of the lattice (bulk) and to various families of Ti^{3+} formed at the surface in relatively disordered environment.[46, 47] The suspension of the rd-TiO_2 in TEOA-thionine solution (Figure 5C(b)) maintain the same EPR feature of the powder (Figure 5C(a)) while the UV-visible irradiation (Figure 5C(c)) causes few modification essentially due to the thionine radical cation. Is more difficult, in this case, to appreciate the change in intensity of the broad signal of Ti^{3+} centers because the sample already contains structural Ti^{3+} center prior irradiation.

Summarizing while TiO_2 and N-TiO_2 show electron trapping ability (as Ti^{3+}) upon illumination of suspension, the same doesn't occur in the case of rd-TiO_2 (a material which is electron rich already before irradiation).

3.4. EPR experiment on TiO_2-impregnated CpHydA systems in TEOA-thionine solution.

The same kind of CW-EPR experiments previously described in Figure 5 and performed on suspensions of bare and modified TiO_2 have been accomplished, in the same experimental conditions, after impregnation of the three supports with the CpHydA protein. The EPR spectra illustrating the behavior of TiO_2-CpHydA , N-TiO_2-CpHydA and rd-TiO_2-CpHydA are reported in Figure 6 (A), (B) and (C) respectively. In Figure 6, for the sake of comparison, the first spectrum (a) of the series (a-d) is always the same, namely that of the H_{ox} state of CpHydA alone in TEOA-thionine solution.
The spectra of the first and second hybrid systems and their behavior under irradiation are similar, at least in qualitative terms and will be discussed together.
The EPR spectra of the as prepared oxidized hybrid systems in dark, Figure 6A(b) and Figure 6B(b), are dominated by the signal of H_{ox}, (compare with Figure 6(a), red spectrum), accompanied by a weaker signal of the H_{ox}-CO species. This particular species represents a byproduct, commonly observed in [FeFe]-hydrogenases spectra, due to the decomposition of the protein: the CO ligands, dissociated from damaged H-clusters, probably bind as free CO molecules to intact H-clusters forming the H_{ox}-CO species.[53] The typical *g* values of CpHydA (H_{ox} state) [50] are g_1 =2.0892, g_2 =2.0363 and g_3 =1.9954 while for H_{ox}-CO the main values are at g =2.075 and g=2.008.[50] The fact that the spectra observed for the surface-anchored protein strictly correspond to those of the free protein, clearly suggests that the active site is not strongly perturbed by the interaction with the oxide and that it likely preserves its local geometry and chemical environment (at least the part of the H-cluster that is monitored by EPR) during the impregnation process and the related treatments.
Irradiation of the two hybrid systems (TiO_2, N-TiO_2) with UV-visible light (Figure 6A(c) and Figure 6B(c)) causes small but significant changes in the EPR spectra. The weak signal due to the H_{ox}-CO species decreases in intensity, in agreement with previous studies,[53, 54] while a new small signal, having a component clearly appreciable at g= 1.93, appears. This signal corresponds to that of the reduced $[2Fe2S]^+$ clusters, with is characterized by *g* values g_1=2.0227 and g_2= 1.936,. Such redox center is peculiar of this type of hydrogenases and it is paramagnetic in reductive conditions.[55, 56] This signal is also detectable upon irradiation of the protein alone and thus it is not an evidence of electron transfer from TiO_2 to the protein. The features of this signal remain visible when the lamp is turned off and maintaining the sample at 77K (data not shown). After a thaw-freeze treatment (RT-77K in dark) the signal due to the reduced $[2Fe2S]^+$ disappears and the features of the EPR spectrum of the oxidized hybrid systems before irradiation are fully recovered (spectra (d) in Figure 6A and Figure 6B).

Rather than the appearance of new weak signal upon irradiation, the most important feature of the sequence of spectra shown in Figure 6A and Figure 6B is that the broad EPR signal, typical of reduced Ti^{3+}centers in irradiated-TiO_2 and N-TiO_2 suspensions (Figure 5), is not observed upon irradiation of the same samples containing the anchored protein. This is a clear evidence of the occurrence of electron transfer from TiO_2 to the protein under irradiation. The photoexcited electrons, in this case, are not stabilized by the matrix as Ti^{3+} ions, but are most likely transferred from the oxide to the protein.

In the case of the rd-TiO_2-CpHydA material things are in part different. Also in this case the main features of the spectrum of the as prepared hybrid system (Figure 6C(b)) are those of the H_{ox} state of the protein. It is worth to note that in the right side of this spectrum only a weak signal of Ti^{3+} ions is observed. However the Ti^{3+} signal is clearly visible in the spectra of rd-TiO_2 both as dry powder and in suspension (Figure 5C(a, b)). This indicates that, upon contact with the protein the reduced Ti^{3+} centers have been oxidized suggesting that excess electrons have been nearly completely scavenged by the protein itself. In Figure 7 the spectrum of the rd-TiO_2 suspension alone is compared to that of the hybrid system rd-TiO_2-CpHydA. From the inspection of this figure is clearly evident that the features of Ti^{3+} in the hybrid system are drastically suppressed. This result is quite amazing if one keeps in mind that the Ti^{3+} centers of rd-TiO_2 are stable in air (i.e. not oxidized by O_2). The electron scavenging ability of the anchored hydrogenase is therefore rather strong.

The UV-Visible irradiation of the rd-TiO_2 sample (Figure 6C(c)) has effects similar to those exhibited by the two other samples. In fact the formation of the signal of reduced $[2Fe2S]^+$ clusters (g= 1.936) is observed again. After a thaw-freeze treatment (Figure 6C(d)) the signals belonging to the $[2Fe2S]^+$ cluster disappear and the EPR spectrum becomes identical to that of the oxidized hybrid systems before irradiation (Figure 6C(b)) confirming the reversibility of the phenomena occurring upon irradiation.

By the way in all hybrid systems tested upon irradiation a slight decrease of the H_{ox} signal intensity is observed suggesting, for a fraction of the protein, a reduction of the active site to an EPR silent form.

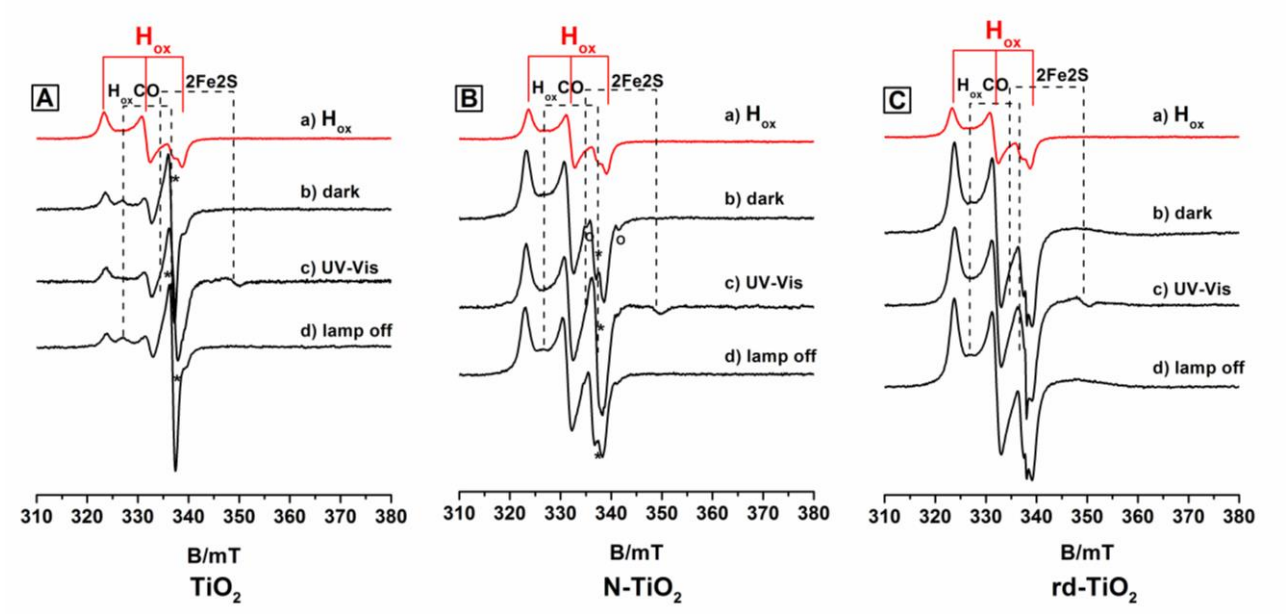

Figure 6. X-band CW-EPR spectra of TiO_2-CpHydA (A), N-TiO_2-CpHydA (B) and rd-TiO_2-CpHydA (C) hybrid systems suspended in TEOA-thionine solution. In all cases the spectrum (a) is that of the CpHydA protein reported for comparison. (b) as prepared oxide-CpHydA hybrid systems in dark; (c) the same system upon irradiation (15 min with UV-visible light); (d) the same sample in (c) upon thaw-freeze treatment in dark (RT-77K).The signals marked by an asterisk are due to the presence of the thionine in the solution (see text), while those marked with circles are signal arising from NO radical trapped in the oxide matrix. All spectra are recorded at T= 77K. **(2 columns fitting image)**

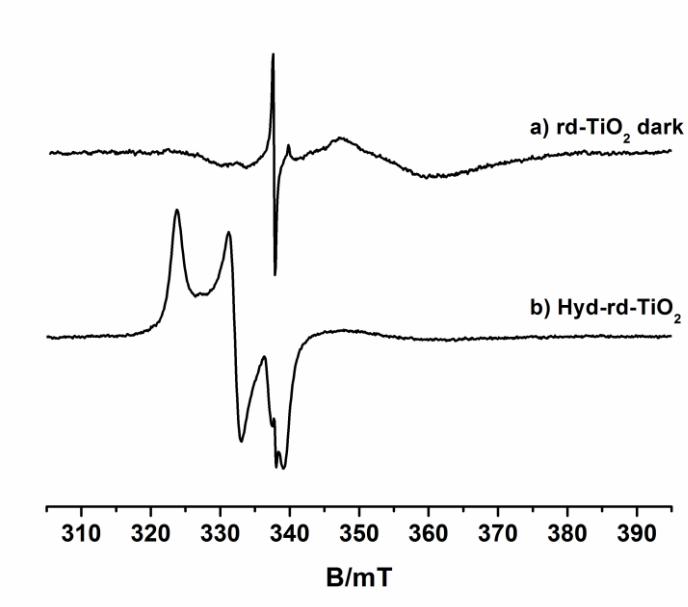

Figure 7. CW-EPR spectra recorded at 77K in dark of rd-TiO_2 suspension (a) and rd-TiO_2-CpHydA systems (b). **(single column fitting image)**

The main results of the present section, based on EPR experiments, can be summarized as follows.

a) Irradiation of a suspension of TiO_2 materials, in the presence of TEOA and thionine, leads, as expected, to the formation of Ti^{3+} centers in the solid because the photogenerated electrons are trapped by Ti^{4+} sites. The holes photogenerated in parallel are annihilated by TEOA. In the case of the substoichiometric, partially reduced, rd-TiO_2 sample (which already contains structural Ti^{3+} center even before irradiation) it is more difficult to appreciate the change in intensity of the Ti^{3+} centers.
b) When contacting the solid support with hydrogenase, the protein interacts with the solid becoming anchored at the surface. In so doing, the features of the protein active site (H-cluster), monitored in terms of EPR spectra of its oxidated form (H_{ox}), remain unchanged. Moreover, in the case of rd-TiO_2, the intensity of the Ti^{3+} signal decreases just upon simple contact with hydrogenase suggesting that a large fraction of the excess electrons in the system are scavenged by the protein. This fact, by the way, confirms that the contact of the protein with the solid is such to allow electron transfer.
c) Irradiation of titania supported hydrogenase at low temperature (77K) causes a (low) decrease in intensity of the H_{ox} signal and, most important, does not induce the formation of reduced Ti^{3+} centers in the solid.

These three facts converge in indicating that the electrons generated by irradiation of the solid are scavenged by the protein even at low temperature and become potentially available for H^+ reduction. With this in mind the photocatalytic activity of the various hybrids in the production of hydrogen under solar irradiation can now be compared.

3.5. Tests on H_2 evolution rate.

In order to obtain a preliminary evaluation of the photocatalytic activity for the TiO_2-based hybrid systems these were submitted to a test of hydrogen evolution under solar light irradiation.

The amount of photogenerated H_2 was measured, via gas chromatography, for the three hybrid systems based on TiO_2, N-TiO_2 and rd-TiO_2 respectively. The corresponding blank tests were performed in the same condition using the oxide supports only.

Figure 7 reports the H_2 evolution rates the three TiO_2-CpHydA hybrid systems in comparison with those of the TiO_2 powders alone. In both cases the powders were suspended in a TEOA solutions and exposed at direct sunlight for 60 minutes. Control experiments performed in the dark or in the absence of TiO_2 did not show any detectable H_2 production (data not shown).

Figure 7 clearly shows that all the hybrid systems present a significantly higher activity in H_2 evolution with respect to that observed for the TiO_2 powders alone.

The turnover frequency numbers (TOF) for these systems are as follows: 2.8 ± 0.2 s^{-1} (TiO_2-CpHydA); 4.1 ± 0.1 s^{-1} (N-TiO-CpHydA_2) and 0.6 ± 0.1 s^{-1} (rd-TiO_2-CpHydA). It is remarkable that the TOF observed here are in good agreement with values observed for CpHydA immobilized on anatase electrodes in an electrochemical cell in the dark.[57] This suggests that binding of CpHydA on various TiO_2 materials and the electron transfer occur similarly. Also, this similarity suggests that, under our conditions, sunlight irradiation is compatible with enzyme function.

A second interesting observation derives from the comparison of the activity of the three hybrid materials. The system based on bare TiO_2 (white) shows, in fact, an intermediate activity between that of the two colored materials. Also taking into account the lower surface area of the rd-TiO_2 sample, its specific activity remains definitively lower than that of the other materials. Remarkably, the introduction of intra band gap states in the TiO_2 band gap obtained via nitrogen doping (N-TiO_2) increase the photoactivity performance of the solid. This means that some more photons of the visible region can be exploited to produce photoexcited electrons, in agreement with recent observation by our group [14] on the mechanism of photoactivity of N-TiO_2. In other words, since the band gap extension is the same for TiO_2 and N-TiO_2, the visible light absorption of the doped sample due to the presence of intra bang gap states is effective for obtaining an increase of the catalytic performance under sun light. The poor activity of rd-TiO_2, in spite of its intense blue color, indicates that the simple coloring does not automatically entail a high photoactivity with visible light. In the case of the rd-TiO_2 such poor activity is likely due to the presence of the high defectivity typical of this kind of heavily reduced materials. Defects in fact can represent recombination centers detrimental for the photoactivity limiting the number of electron available for the H^+ reducing at the protein active site.

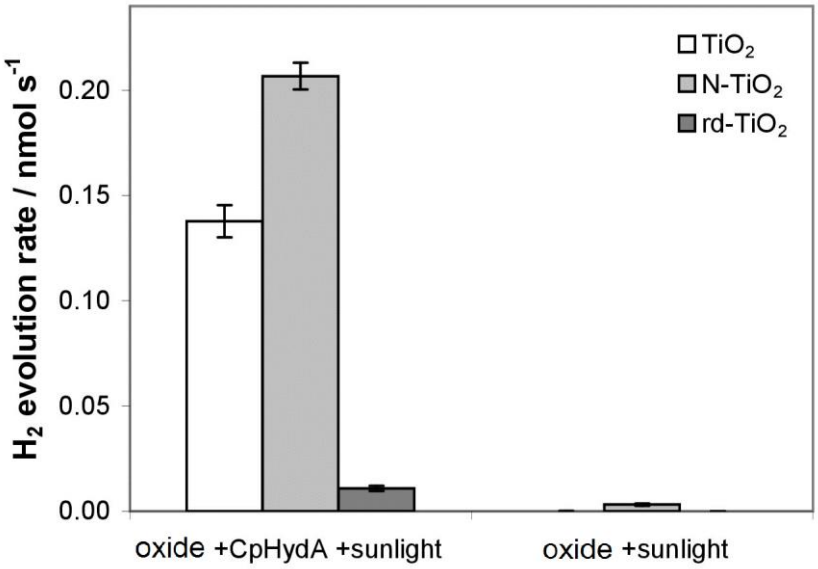

Figure 7. H_2 evolution tests. Different TiO_2 powder systems (1mg/ml) impregnated with CpHydA (50nM) or alone in TEOA solutions irradiated with natural sunlight. Left hand side: hybrid systems. Right hand side: only oxide. The error bars refer to triplicate standard deviation. **(single column fitting image)**

4. Conclusions

We have characterized for the first time by EPR spectroscopy the behavior of different TiO_2-CpHydA hybrid systems under irradiation. The experiments reported in this paper demonstrate that the various treatments undergone by the protein along the anchoring on the TiO_2 powder seem not affect the H-cluster geometry and the catalytic capability of the protein.

Furthermore, the experiments shown in Figure 6 show that the hydrogenase molecule in the hybrid system is indeed a scavenger of photoexcited electrons, in fact these are no more trapped by Ti^{4+} centers as it occurs in the case of the oxide supports in the absence of the protein (Figure 5).

This result is relevant as it definitely shows that hydrogenase after surface anchoring on TiO_2, is in electronic contact with the solid thus allowing the electron transfer and the H^+ reduction.

In terms of photocatalytic activity the present work remains a proof of concept. The H_2 evolution tests, however, shows that, in spite of a quite modest production of H_2, the hybrid system could have a strong potential in this field since the functionalization of TiO_2 with the protein sustains an H_2 evolution rate at least one order of magnitude higher than that of the TiO_2 powder alone.

Finally, the N-TiO_2-CpHydA sample exhibits the highest activity among all hybrid systems tested in this work. This is due to the presence of intra band gap levels 2.5 eV below the conduction band that, as previously shown by some of us,[13-15] are available to excite the electrons of the valence band

to the conduction band even under visible light. This allows the employment of a fraction of photons present in the solar light [14] which are not effective in the case of bare TiO_2. To conclude, once demonstrated the potential of oxide supported hydrogenase in H_2 photoproduction, the search for an optimal solid matrix to improve the photocatalytic performance under sunlight is now open.

Acknowledgements

This work has been supported by the CARIPLO Fondation through the grant n° 2013-0615 "Novel heterojunction based photocatalytic materials for solar energy conversion" The support of the COST Action CM1104 “Reducible oxide chemistry, structure and functions” is also gratefully acknowledged. Funding from project BIOTHYTAN (E.U. Structural Funds N.1083/2006 F.E.S.R. 2007-2013) is also acknowledged.

References

[1] Fujishima A, Honda K. Electrochemical photolysis of water at a semiconductor electrode. Nature. 1972;238:37-8.
[2] Linsebigler AL, Lu GQ, Yates JT. Photocatalysis on TiO_2 surfaces - principles, mechanisms, and selected results. Chemical Reviews. 1995;95:735-58.
[3] Ireland JC, Klostermann P, Rice EW, Clark RM. Inactivation of *escherichia-coli* by titanium-dioxide photocatalytic oxidation. Applied and Environmental Microbiology. 1993;59:1668-70.
[4] Cho M, Chung H, Choi W, Yoon J. Linear correlation between inactivation of *E-coli* and OH radical concentration in TiO_2 photocatalytic disinfection. Water Research. 2004;38:1069-77.
[5] Nozawa M, Tanigawa K, Hosomi M, Chikusa T, Kawada E. Removal and decomposition of malodorants by using titanium dioxide photocatalyst supported on fiber activated carbon. Water Science and Technology. 2001;44:127-33.
[6] Mellott NP, Durucan C, Pantano CG, Guglielmi M. Commercial and laboratory prepared titanium dioxide thin films for self-cleaning glasses: Photocatalytic performance and chemical durability. Thin Solid Films. 2006;502:112-20.
[7] Maeda K, Domen K. Photocatalytic Water Splitting: Recent Progress and Future Challenges. Journal of Physical Chemistry Letters. 2010;1:2655-61.
[8] Hisatomi T, Kubota J, Domen K. Recent advances in semiconductors for photocatalytic and photoelectrochemical water splitting. Chemical Society Reviews. 2014;43:7520-35.
[9] Palmisano L, Augugliaro V, Bellardita M, Di Paola A, Lopez EG, Loddo V, et al. Titania Photocatalysts for Selective Oxidations in Water. Chemsuschem. 2011;4:1431-8.
[10] Youngblood WJ, Lee S-HA, Maeda K, Mallouk TE. Visible Light Water Splitting Using Dye-Sensitized Oxide Semiconductors. Accounts of Chemical Research. 2009;42:1966-73.
[11] Li H, Bian Z, Zhu J, Huo Y, Li H, Lu Y. Mesoporous Au/TiO_2 nanocomposites with enhanced photocatalytic activity. Journal of the American Chemical Society. 2007;129:4538-9.
[12] Zielinska-Jurek A, Kowalska E, Sobczak JW, Lisowski W, Ohtani B, Zaleska A. Preparation and characterization of monometallic (Au) and bimetallic (Ag/Au) modified-titania photocatalysts activated by visible light. Applied Catalysis B-Environmental. 2011;101:504-14.
[13] Livraghi S, Paganini MC, Giamello E, Selloni A, Di Valentin C, Pacchioni G. Origin of photoactivity of nitrogen-doped titanium dioxide under visible light. Journal of the American Chemical Society. 2006;128:15666-71.

[14] Barolo G, Livraghi S, Chiesa M, Paganini MC, Giamello E. Mechanism of the Photoactivity under Visible Light of N-Doped Titanium Dioxide. Charge Carriers Migration in Irradiated N-TiO_2 Investigated by Electron Paramagnetic Resonance. Journal of Physical Chemistry C. 2012;116:20887-94.
[15] Livraghi S, Chierotti MR, Giamello E, Magnacca G, Paganini MC, Cappelletti G, et al. Nitrogen-Doped Titanium Dioxide Active in Photocatalytic Reactions with Visible Light: A Multi-Technique Characterization of Differently Prepared Materials. Journal of Physical Chemistry C. 2008;112:17244-52.
[16] Sacco O, Stoller M, Vaiano V, Ciambelli P, Chianese A, Sannino D. Photocatalytic Degradation of Organic Dyes under Visible Light on N-Doped TiO_2 Photocatalysts. International Journal of Photoenergy. 2012.
[17] Livraghi S, Elghniji K, Czoska AM, Paganini MC, Giamello E, Ksibi M. Nitrogen-doped and nitrogen-fluorine-codoped titanium dioxide. Nature and concentration of the photoactive species and their role in determining the photocatalytic activity under visible light. Journal of Photochemistry and Photobiology a-Chemistry. 2009;205:93-7.
[18] Wang Q, Chen C, Ma W, Zhu H, Zhao J. Pivotal Role of Fluorine in Tuning Band Structure and Visible-Light Photocatalytic Activity of Nitrogen-Doped TiO_2. Chemistry-a European Journal. 2009;15:4765-9.
[19] Vaiano V, Sacco O, Sannino D, Ciambelli P, Longo S, Venditto V, et al. N-doped TiO_2/s-PS aerogels for photocatalytic degradation of organic dyes in wastewater under visible light irradiation. Journal of Chemical Technology and Biotechnology. 2014;89:1175-81.
[20] Vaiano V, Sacco O, Sannino D, Ciambelli P. Process intensification in the removal of organic pollutants from wastewater using innovative photocatalysts obtained coupling Zinc Sulfide based phosphors with nitrogen doped semiconductors. Journal of Cleaner Production. 2015;100:208-11.
[21] Vaiano V, Sacco O, Stoller M, Chianese A, Ciambelli P, Sannino D. Influence of the Photoreactor Configuration and of Different Light Sources in the Photocatalytic Treatment of Highly Polluted Wastewater. International Journal of Chemical Reactor Engineering. 2014;12:63–75.
[22] Kim S, Lu D, Park S, Wang G. Production of hydrogenases as biocatalysts. International Journal of Hydrogen Energy. 2012;37:15833-40.
[23] Lubitz W, Ogata H, Ruediger O, Reijerse E. Hydrogenases. Chemical Reviews. 2014;114:4081-148.
[24] Vignais PM, Billoud B. Occurrence, classification, and biological function of hydrogenases: An overview. Chemical Reviews. 2007;107:4206-72.
[25] Fontecilla-Camps JC, Volbeda A, Cavazza C, Nicolet Y. Structure/function relationships of [NiFe]- and [FeFe]-hydrogenases. Chemical Reviews. 2007;107:4273-303.
[26] King PW. Designing interfaces of hydrogenase-nanomaterial hybrids for efficient solar conversion. Biochimica Et Biophysica Acta-Bioenergetics. 2013;1827:949-57.
[27] Reisner E. Solar Hydrogen Evolution with Hydrogenases: From Natural to Hybrid Systems. European Journal of Inorganic Chemistry. 2011:1005-16.
[28] Reisner E, Powell DJ, Cavazza C, Fontecilla-Camps JC, Armstrong FA. Visible Light-Driven H_2 Production by Hydrogenases Attached to Dye-Sensitized TiO_2 Nanoparticles. Journal of the American Chemical Society. 2009;131:18457-66.
[29] Morra S, Valetti F, Sadeghi SJ, King PW, Meyer T, Gilardi G. Direct electrochemistry of an [FeFe]-hydrogenase on a TiO_2 Electrode. Chemical Communications. 2011;47:10566-8.
[30] Nikandrov VV, Shlyk MA, Zorin NA, Gogotov IN, Krasnovsky AA. Efficient photoinduced electron-transfer from inorganic semiconductor TiO_2 to bacterial hydrogenase. Febs Letters. 1988;234:111-4.
[31] Cuendet P, Rao KK, Gratzel M, Hall DO. Light-induced H_2 evolution in a hydrogenase-TiO_2 particle system by direct electron-transfer or via Rhodium complexes. Biochimie. 1986;68:217-21.
[32] Caputo CA, Wang L, Beranek R, Reisner E. Carbon nitride-TiO_2 hybrid modified with hydrogenase for visible light driven hydrogen production. Chemical Science. 2015;6:5690-4.
[33] Livraghi S, Votta A, Paganini MC, Giamello E. The nature of paramagnetic species in nitrogen doped TiO_2 active in visible light photocatalysis. Chemical Communications. 2005:498-500.
[34] Liu G, Yang HG, Wang X, Cheng L, Lu H, Wang L, et al. Enhanced Photoactivity of Oxygen-Deficient Anatase TiO_2 Sheets with Dominant {001} Facets. Journal of Physical Chemistry C. 2009;113:21784-8.
[35] Liu L, Chen X. Titanium Dioxide Nanomaterials: Self-Structural Modifications. Chemical Reviews. 2014;114:9890-918.

[36] Liu X, Gao S, Xu H, Lou Z, Wang W, Huang B, et al. Green synthetic approach for Ti^{3+} self-doped TiO_{2-x} nanoparticles with efficient visible light photocatalytic activity. Nanoscale. 2013;5:1870-5.
[37] Zhang H, Zhao Y, Chen S, Yu B, Xu J, Xu H, et al. Ti^{3+} self-doped TiO_x@anatase core-shell structure with enhanced visible light photocatalytic activity. Journal of Materials Chemistry A. 2013;1:6138-44.
[38] Su J, Zou X, Chen J-S. Self-modification of titanium dioxide materials by Ti^{3+} and/or oxygen vacancies: new insights into defect chemistry of metal oxides. Rsc Advances. 2014;4:13979-88.
[39] Zuo F, Wang L, Wu T, Zhang Z, Borchardt D, Feng P. Self-Doped Ti^{3+} Enhanced Photocatalyst for Hydrogen Production under Visible Light. Journal of the American Chemical Society. 2010;132:11856-7.
[40] Khomenko VM, Langer K, Rager H, Fett A. Electronic absorption by Ti^{3+} ions and electron delocalization in synthetic blue rutile. Physics and Chemistry of Minerals. 1998;25:338-46.
[41] Silakov A, Reijerse EJ, Albracht SPJ, Hatchikian EC, Lubitz W. The electronic structure of the H-cluster in the [FeFe]-hydrogenase from *Desulfovibrio desulfuricans*: A Q-band Fe-57-ENDOR and HYSCORE study. Journal of the American Chemical Society. 2007;129:11447-58.
[42] Silakov A, Wenk B, Reijerse E, Albracht SPJ, Lubitz W. Spin distribution of the H-cluster in the H_{ox}-CO state of the [FeFe] hydrogenase from *Desulfovibrio desulfuricans*: HYSCORE and ENDOR study of ^{14}N and ^{13}C nuclear interactions. Journal of Biological Inorganic Chemistry. 2009;14:301-13.
[43] Mulder DW, Ratzloff MW, Shepard EM, Byer AS, Noone SM, Peters JW, et al. EPR and FTIR Analysis of the Mechanism of H_2 Activation by [FeFe]-Hydrogenase *HydA1* from *Chlamydomonas reinhardtii*. Journal of the American Chemical Society. 2013;135:6921-9.
[44] Bennett B, Lemon BJ, Peters JW. Reversible carbon monoxide binding and inhibition at the active site of the Fe-only hydrogenase. Biochemistry. 2000;39:7455-60.
[45] von Abendroth G, Stripp S, Silakov A, Croux C, Soucaille P, Girbal L, et al. Optimized over-expression of [FeFe] hydrogenases with high specific activity in *Clostridium acetobutylicum*. International Journal of Hydrogen Energy. 2008;33:6076-81.
[46] Livraghi S, Chiesa M, Paganini MC, Giamello E. On the nature of reduced states in titanium dioxide as monitored by electron paramagnetic resonance. I: The anatase case. Journal of Physical Chemistry C. 2011;115:25413-21.
[47] Chiesa M, Paganini MC, Livraghi S, Giamello E. Charge trapping in TiO_2 polymorphs as seen by Electron Paramagnetic Resonance spectroscopy. Physical Chemistry Chemical Physics. 2013;15:9435-47.
[48] Livraghi S, Rolando M, Maurelli S, Chiesa M, Paganini MC, Giamello E. Nature of reduced states in titanium dioxide as monitored by electron paramagnetic resonance. II: Rutile and brookite cases. Journal of Physical Chemistry C. 2014;118:22141-8.
[49] Morra S, Arizzi M, Allegra P, La Licata B, Sagnelli F, Zitella P, et al. Expression of different types of [FeFe]-hydrogenase genes in bacteria isolated from a population of a bio-hydrogen pilot-scale plant. International Journal of Hydrogen Energy. 2014;39:9018-27.
[50] Morra S, Mongili B, Maurelli S, Gilardi G, Valetti F. Isolation and characterization of a new [FeFe]-hydrogenase from *Clostridium perfringens*. Biotechnology and Applied Biochemistry. 2015:1-7.
[51] Hagen WR, Wassink H, Eady RR, Smith BE, Haaker H. Quantitative EPR of an s = 7/2 system in thionine-oxidized mofe proteins of nitrogenase. A redefinition of the p-cluster concept. European Journal of Biochemistry. 1987;169:457-65.
[52] Katafias A, Fenska J. Sulfuric acid controlled oxidative degradation of azure B and thionine dyes by cerium(IV). International Journal of Chemical Kinetics. 2011;43:523-36.
[53] Albracht SPJ, Roseboom W, Hatchikian EC. The active site of the [FeFe]-hydrogenase from *Desulfovibrio desulfuricans*. 1. Light sensitivity and magnetic hyperfine interactions as observed by electron paramagnetic resonance. Journal of Biological Inorganic Chemistry. 2006;11:88-101.
[54] Kowal AT, Adams MWW, Johnson MK. Electron-Paramagnetic Resonance studies of the low-temperature photolytic behavior of oxidized hydrogenase I from *clostridium-pasteurianum*. Journal of Biological Chemistry. 1989;264:4342-8.
[55] Morra S, Maurelli S, Chiesa M, Mulder DW, Ratzloff MW, Giamello E, et al. The effect of a C298D mutation in CaHydA [FeFe]-hydrogenase: Insights into the protein-metal cluster interaction by EPR and FTIR spectroscopic investigation. Biochimica et Biophysica Acta - Bioenergetics. 2016;1857:98-106.

[56] Mitou G, Higgins C, Wittung-Stafshede P, Conover RC, Smith AD, Johnson MK, et al. An Isc-type extremely thermostable [2Fe-2S] ferredoxin from Aquifex aeolicus. Biochemical, spectroscopic, and unfolding studies. Biochemistry. 2003;42:1354-64.
[57] Morra S, Valetti F, Sarasso V, Castrignano S, Sadeghi SJ, Gilardi G. Hydrogen production at high Faradaic efficiency by a bio-electrode based on TiO_2 adsorption of a new [FeFe]-hydrogenase from *Clostridium perfringens*. Bioelectrochemistry. 2015;106:258-62.

Grafical abstract